ISSN 0030-400X, Optics and Spectroscopy, 2021, Vol. 129, No. 12, pp. 1306–1310. © Pleiades Publishing, Ltd., 2021.
ISSN 0030-400X, Optics and Spectroscopy, 2021. © Pleiades Publishing, Ltd., 2021.
Russian Text © The Author(s), 2021, published in Optika i Spektroskopiya, 2021, Vol. 129, No. 9, pp. 1183–1187.

Optical and Structural Properties of Palladium Nanofilms in Hydrogen Atmosphere

V. A. Shutaev[a], *, V. A. Matveev[b], E. A. Grebenshchikova[a], V. G. Shchelokov[a], and Yu. P. Yakovlev[a]

[a] *Ioffe Institute, Russian Academy of Sciences, St. Petersburg, 194021 Russia*
[b] *Peterburg Nuclear Physics Institute, National Research Center "Kurchatov Institute," Gatchina, Leningrad oblast, 188300 Russia*
**e-mail: vadimshutaev@mail.ru*

Received March 11, 2021; revised March 11, 2021; accepted March 31, 2021

Abstract—The crystal structure and optical properties of Pd thin films (thickness 10–130 nm) obtained by thermal deposition in vacuum are studied. It is shown that the Pd films are polycrystalline and the average size of crystallites depends on the film thickness. The transparency of films at a wavelength of 0.95 μm is studied in air and hydrogen (100%) atmospheres. It is experimentally found that the optical transparency of Pd films with thicknesses in the range of 10–45 nm obeys the Bouguer law in both air and hydrogen atmospheres. The thickness range of Pd films suitable for practical application in hydrogen sensors is determined experimentally.

Keywords: palladium, hydrogen, optical transparency, crystallites, nanofilms

DOI: 10.1134/S0030400X21090204

1. INTRODUCTION

The palladium–hydrogen system has been extensively studied for many years [1]. Palladium (Pd), which is a platinum group metal, has some properties owing to which it finds application in various fields of industry. The high catalytic activity (especially in the finely dispersed state) and the unique ability of Pd to efficiently dissolve hydrogen makes it possible to use this metal as an active element in hydrogen sensors [2]. When dissolving in metal, hydrogen occupies interstitial sites and stretches the lattice. In addition, the embedded atom causes distortions of the surrounding metal lattice [3]. Some Pd properties, such as conductivity and optical transparency, change as a result of hydrogen adsorption. In particular, we observed in [4] an abrupt increase in the transparency of Pd layers at a hydrogen concentration between 1 and 10%, which is typical for the first-order phase transitions. In this case, the rate of changes in the layer transparency linearly increased with increasing concentration of hydrogen in the gas medium.

Palladium films formed by different methods may differ in the size of Pd crystallites and may additionally contain palladium oxide, because of which they can have different physical and chemical properties [5, 6]. It was noted in [7] that the use of nanosized semiconductor materials for gas sensorics provides a higher sensitivity than the bulk materials due to the higher surface-to-volume ratio. This means that a considerable fraction of these systems consists of surface atoms, which can participate in near-surface reactions. The authors of [8] claim that the specific surface value is important not only from the chemical but also from the physical points of view. To provide measurable sensor signals, the change in the electroconductivity due to the surface processes should be of the same order as the semiconductor electroconductivity. This means that the contribution of the surface to the electrophysical parameters of the material should be comparable with the contribution from the volume. In the opinion of the authors of [8], a promising material should have a crystallite size of 5–20 nm and a specific surface of up to 100–200 m^2/g. At the same time, materials with the size of particles exceeding 0.5 μm almost do not exhibit sensor properties.

The present work continues the study of the optical transparency of Pd films in a hydrogen atmosphere. The aim of this work is to study the influence of hydrogen on the optical and structural properties of Pd nanofilms in a hydrogen atmosphere.

2. EXPERIMENTAL

The Pd layers were formed by thermal evaporation in vacuum at a residual pressure of 10^{-6} Torr on glass substrates 1.5 mm thick (object glass). The glass substrate was positioned on a table heated to 100°C. The

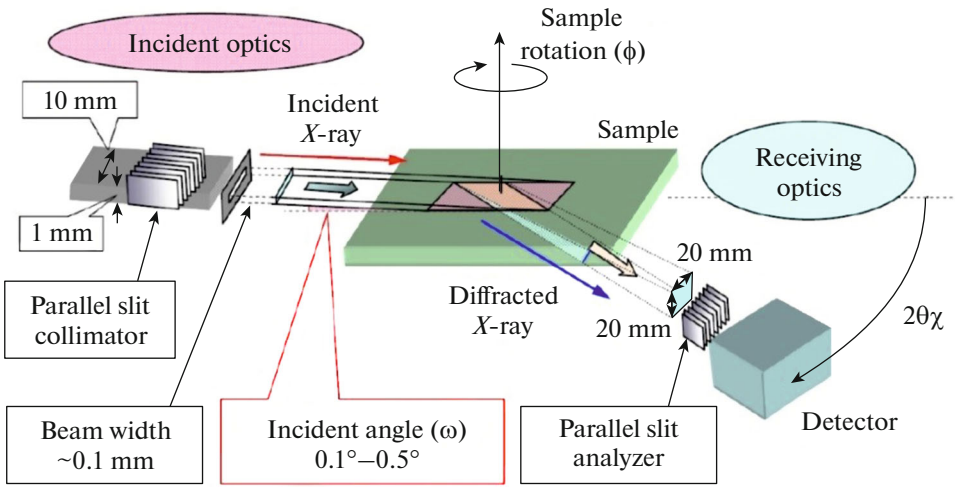

Fig. 1. Scheme of the X-ray diffraction experiment in the in-plane geometry.

deposition method was similar to the technology of deposition of Pd layers in Pd/oxide/InP structures [9, 10]. The thickness of films formed was measured using a Dektak 3030 profilometer and X-ray reflectometry.

The transparency of layers was measured at room temperature at a wavelength of 0.95 μm on an MDR-2 monochromator with a silicon photodetector. The absorption of light in the glass substrate did not exceed 2% and was taken into account when processing the spectra. The measurements were performed in air and hydrogen (100%) atmospheres.

The X-ray diffraction patterns were taken in the Bragg–Brentano scheme (θ/2θ) and at grazing incidence of a parallel X-ray beam. The X-ray patterns in the Bragg–Brentano geometry were recorded on a DRON-3 diffractometer (Burevestnik, Russia).

Recording conditions were as follows: radiation Cu$K\alpha$, tube voltage 36 kV, current 24 mA, counter rotation rate 2 deg/min, electronic recording system. The X-ray diffraction patterns were processed using a PDWin software (Burevestnik, Russia).

The crystal structure of palladium films with thicknesses of 10–130 nm was studied by grazing incidence X-ray diffraction (GIXRD). The diffraction patterns were recorded using a Rigaku SmartLab diffractometer (Cu$K\alpha$, 45 kW, 200 mA) in the in-plane geometry, in which a quasi-parallel X-ray beam formed by a parallel-slit collimator was incident on the sample surface at a fixed grazing angle $\omega = 0.6°$ (Fig. 1). The detector was rotated with respect to the ω axis, which was perpendicular to sample plane, and the sample itself was also rotated around the same axis. To increase the diffractometer resolution, a parallel slit analyzer was positioned in front of the detector.

3. RESULTS AND DISCUSSION

3.1. Analysis of Diffraction Patterns Obtained in the Bragg–Brentano Geometry

Figure 2a presents diffraction patterns for Pd film with different thicknesses, which were recorded by the Bragg–Brentano scheme. Recording was performed from the coated surface of samples and, in one case (for sample 3), additionally from the opposite (uncoated) side of glass. All diffraction patterns of coated samples contain broad peaks corresponding to amorphous glass. The film on sample 1 is partially dropped and partially remained on the glass. Recording was performed from the sample region with the remained film. The diffraction pattern of the Pd film 130 nm thick (curve *1* in Fig. 2) exhibits three clear peaks of crystalline palladium (PDF-2 no. 46-1043). From Fig. 2, one can only conclude that the Pd film with a thickness of 130 nm (sample 1), which is ten times higher than the film thickness of sample 3, has a crystalline structure. For thinner films (13 and 30 nm), this method yields no information, because of which, to study the structure of these samples, we recorded diffraction patterns in the grazing-incidence geometry.

3.2. Analysis of Diffraction Patterns Obtained by Grazing Incidence X-Ray Diffraction

The diffraction patterns obtained by grazing incidence X-ray diffraction for Pd films with different thicknesses are presented in Fig. 3. The diffraction patterns clearly show Bragg peaks corresponding to the (111), (200), (220), (311), and (222) families of planes of the face-centered cubic Pd lattice (ICSD 064920). Thus, the Pd films are polycrystalline. The

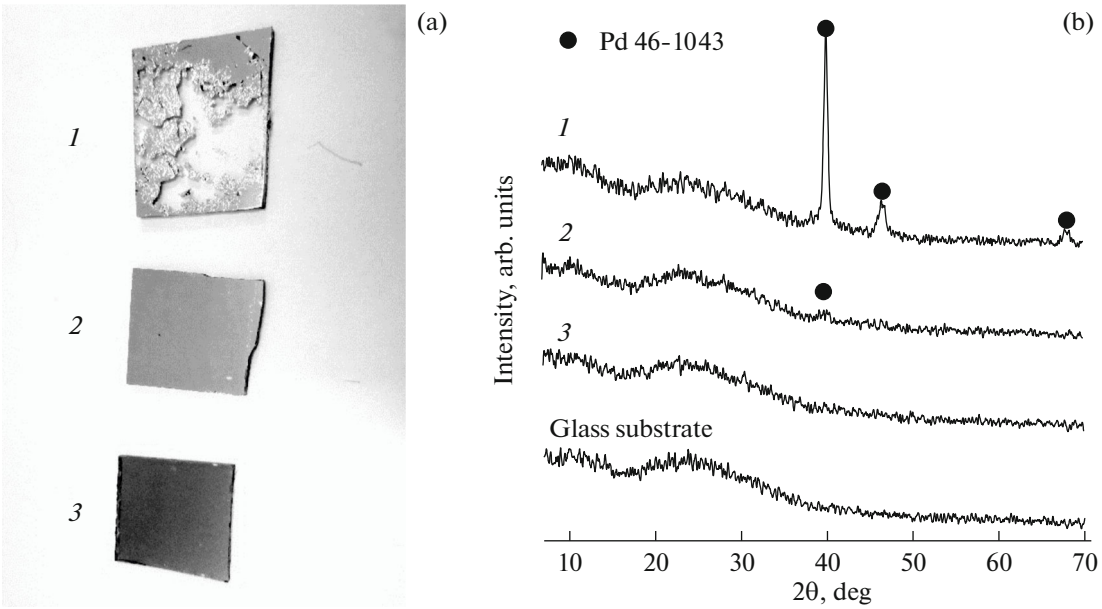

Fig. 2. (a) Photographs and (b) Bragg–Brentano diffraction patterns of samples with Pd films (*1*) 130, (*2*) 30, and (*3*) 13 nm thick.

diffraction patterns did not contain Bragg peaks of palladium oxide.

The sizes of crystallites in films were determined using the Scherrer formula [11]

$$\beta = \frac{K\lambda}{D_{cr}\cos\theta},$$

where β is the Bragg peak broadening, $K = 0.9$ is the form-factor of particles (crystallites), $\lambda = 0.15406$ nm is the X-ray radiation wavelength, D_{cr} is the average size of crystallites, and θ is the angle of incidence of the X-ray beam. It is necessary to note that the instrumental broadening also contributes to the broadening of diffraction peaks. However, due to a small size of crystallites and, as a result, a large width of diffraction peaks, this contribution can be neglected.

Figure 4 shows the dependence of the average size of crystallites D_{cr} on the palladium film thickness d, which is obtained as a result of processing of diffraction patterns. As is seen from the dependence, the average size of crystallites increases with increasing thickness of the Pd film. Similar increase was also observed in the case of other metals, for example, for platinum and gold films [12].

Thus, by assigning the Pd film thickness, one can obtain crystallites of a desired size. For films with thicknesses from 10 to 50 nm, it is possible to obtain crystallites with an average size of 5–10 nm, which allows one to achieve a large specific surface and a strong sensor signal [7, 8].

3.3. Influence of Hydrogen on the Optical Transparency of Palladium Films with Different Thicknesses (10–80 nm)

Figure 5 shows the measured dependences of the transparency of Pd layers at a wavelength of 0.95 μm on their thickness in air and hydrogen atmospheres. To emphasize the influence of hydrogen on the transparency of Pd layers, we present the dependences of the transparency of palladium layers on their thickness on both linear and semilogarithmic scales.

It was previously experimentally shown that the character of the transparency spectra of Pd layers in the studied range of thicknesses, as well as the transparency peak position (0.95 μm), are independent of the sample thickness [4]. It was shown that the films with thicknesses of 10–45 nm in air obey the Bouguer law and then, beginning from the Pd layer thickness exceeding 45 nm, the transparency of films decreases linearly rather than according to Bouguer law.

Let us represent the photoelectromotive force (which is proportional to the optical transparency of palladium films) measured by a photodetector behind the sample by the formula

$$U = U_0 \exp(-\alpha d),$$

where U_0 and U are the photoelectromotive forces without and with the sample, d is the layer thickness, and α is the absorption coefficient of Pd. We assume that the photoelectromotive force is proportional to the intensities of light incident on the sample and

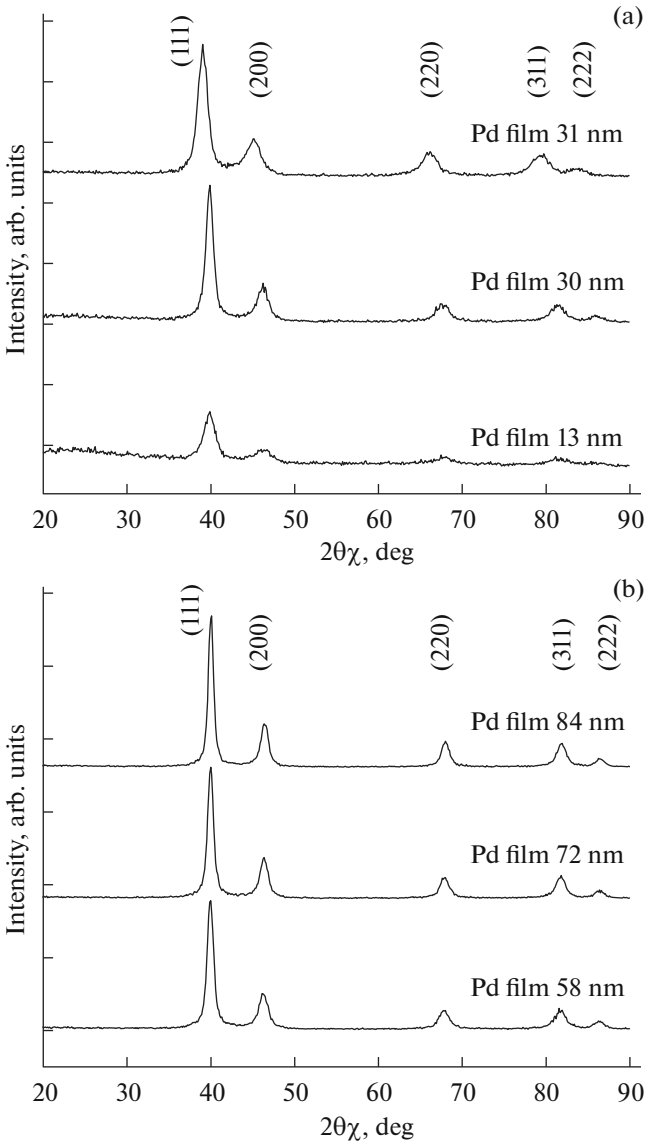

Fig. 3. Diffraction patterns of Pd films with different thicknesses.

transmitted through it. The absorption coefficient α can be written as

$$\alpha = -\frac{\ln\frac{U}{U_0}}{d}.$$

One can see from Fig. 5 that the absorption coefficient of samples obeying the Bouguer law decreases by a factor of 1.9 under action of hydrogen. This coefficient is 11.7×10^4 cm^{-1} in air and 6.5×10^4 cm^{-1} in hydrogen. The maximum change in the transparency under action of hydrogen is observed in films with thicknesses of 30–40 nm.

It should be noted that the average size of crystallites D_{cr} in these Pd layers is 7–10 nm, which is com-

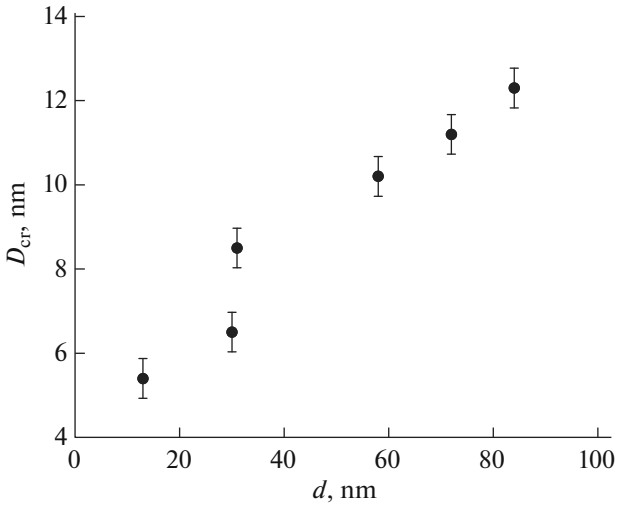

Fig. 4. Dependence of average size of crystallites D_{cr} on palladium film thickness d.

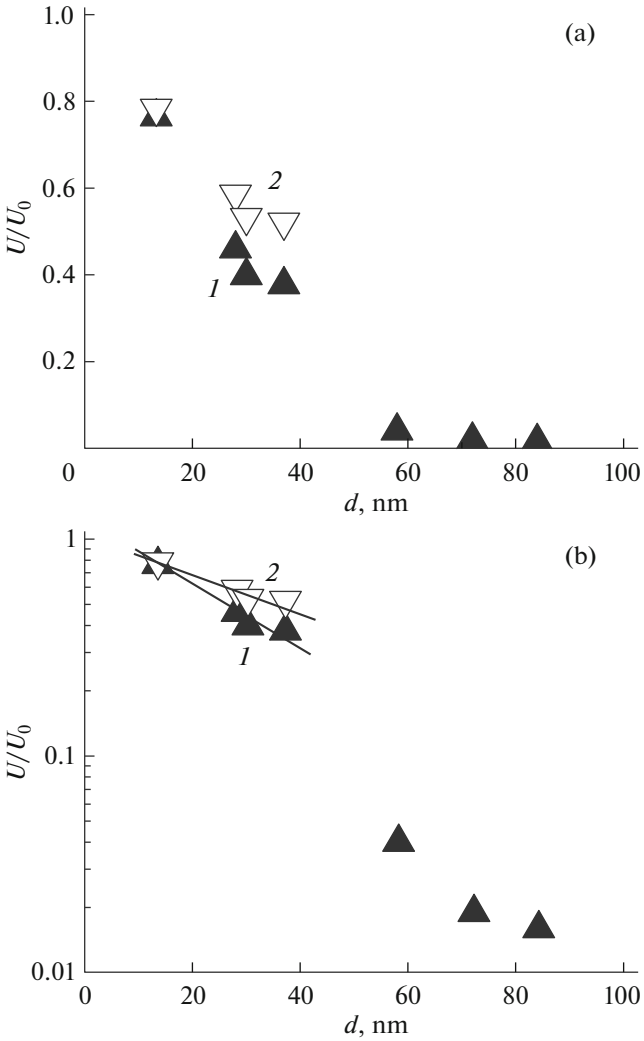

Fig. 5. Dependences of the transparency of Pd layers (λ = 0.95 μm) on their thicknesses in (*1*) air (α = 11.7×10^4 cm^{-1}) and (*2*) hydrogen (α = 6.5×10^4 cm^{-1}) on the (a) linear and (b) semilogarithmic scales.

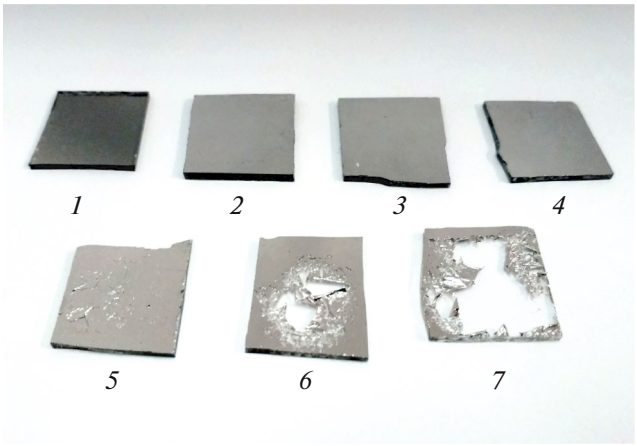

Fig. 6. Photographs of samples with Pd films (*1*) 13, (*2*) 30, (*3*) 31, (*4*) 58, (*5*) 72, (*6*) 84, and (*7*) 130 nm thick, which were thermally deposited in vacuum on glass substrates, after action of 100% hydrogen.

parable with palladium grains in films obtained by electrophoresis and electron beam deposition [6, 7, 12]. It can be said that the properties of Pd films with these sizes of Pd crystallites are isomorphous because the polycrystalline metal grains are extremely small in comparison with the sample and are randomly distributed; thus, all orientations of grains are equally probable, and, on average, the film properties are identical for all directions. It is also necessary to note that these samples retain their plasticity and form after multiple action of hydrogen (Fig. 6).

Palladium films with thicknesses exceeding 45 nm demonstrate a deviation from the Bouguer law in air and are destroyed in the hydrogen atmosphere. The size of crystallites abruptly changes approximately at the same thickness, which follows from the dependence shown in Fig. 4.

At a steady-state measurement regime, we observed partial detachment of films with thicknesses of ≥50 nm from the substrate (Fig. 6). An increase in the size of palladium crystallites obviously causes elastic stresses in the metal structure, which leads to destruction of films under the action of hydrogen with high concentrations, at which Pd transforms into PdH_x ($x > 0.6$). This agrees well with the studies described in [13].

4. CONCLUSIONS

It is shown that the Pd films formed by thermal deposition in vacuum are polycrystalline and the average size of Pd crystallites correlates with the film thickness. The range of film thicknesses at which the action of hydrogen with a 100% concentration does not cause destruction of films is determined experimentally. The optical transparency of films obtained is studied. It is found that, in the studied thickness region (10–100 nm), the maximum increase in the film transparency due to a replacement of the atmosphere air for 100% hydrogen occurs at a Pd layer thickness of about 30–40 nm. The films with this thickness are promising for application in optical hydrogen sensors.

CONFLICT OF INTEREST

The authors declare that they have no conflict of interest.

REFERENCES

1. F. A. Lewis, Platinum Met. Rev. **26**, 20 (1982).
2. T. Hubert, L. Boon-Brett, and G. Banach, Sens. Actuators, B **157**, 329 (2011).
3. Yu. M. Koroteev, O. V. Gimranova, and I. P. Chernov, Phys. Solid State **53**, 896 (2011).
4. V. A. Shutaev, E. A. Grebenshchikova, V. G. Sidorov, and Yu. P. Yakovlev, Opt. Spectrosc. **128**, 596 (2020). https://doi.org/10.1134/S0030400X20050148
5. Y.-I. Chou, Ch.-M. Chen, W.-Ch. Liu, and H.-I. Chen, IEEE Electron Device Lett. **26**, 62 (2005). https://doi.org/10.1109/LED.2004.840736
6. J. Grym, O. Procházková, R. Yatskiv, et al., Nanoscale Res. Lett. **6**, 392 (2011). https://doi.org/10.1186/1556-276X-6-392
7. T. V. Peshkova, D. Ts. Dimitrov, S. S. Nalimova, I. E. Kononova, N. K. Nikolaev, K. I. Papazova, A. S. Bozhinova, V. A. Moshnikov, and E. I. Terukov, Tech. Phys. **59**, 771 (2014).
8. A. V. Marikutsa, M. N. Rumyantseva, and A. M. Gas'kov, *Nanomaterials: Properties and Promising Applications,* Ed. by A. B. Yaroslavtsev (Nauchnyi Mir, Moscow, 2014) [in Russian].
9. V. A. Shutaev, E. A. Grebenshchikova, A. A. Pivovarova, V. G. Sidorov, L. K. Vlasov, and Yu. P. Yakovlev, Semiconductors **53**, 1389 (2019).
10. E. A. Grebenshchikova, V. G. Sidorov, V. A. Shutaev, and Yu. P. Yakovlev, Semiconductors **53**, 234 (2019).
11. A. L. Patterson, Phys. Rev. **56**, 978 (1939).
12. L. L. Melo, A. R. Vaz, M. C. Salvadori, and M. Cattani, J. Metastable Nanocryst. Mater. **20–21,** 623 (2004).
13. G. I. Zhirov, Fiz. Tekh. Vys. Davl. **13** (2), 71 (2003).

Translated by M. Basieva